Hydrodynamic Studies of Post Dryout Two-Phase Downflow in Narrow Channels

by

Cris S. Eberle

Argonne National Laboratory
P.O. Box 2528
Idaho Falls, ID 83403

M. Ishii
and
S. T. Revankar

Purdue University
1290 Nuclear Engineering Building
West Lafayette, IN 47907

The Thirtieth ASME/AIChE/ANS/AIAA, National Heat Transfer Conference,
Portland, Oregon

August 5-9, 1995

ABSTRACT

An experimental study of the hydrodynamics of a narrow channel was performed in order to obtain the heat transfer mechanisms and influences contributing to the flow regime transition from inverted annular to inverted slug flows for post dryout downflow. The experimental series consisted of both adiabatic and diabatic visualization tests over a wide range of fluid and thermal parameters. The system inlet gas velocities ranged from 0 to 14 meters per second while the inlet fluid velocities ranged from 1 to 3 meters per second. Full extent visualization of the flow regime was possible due to a quartz tube in tube construction with a clear heating fluid. Constant temperature heating of the freon was accomplished at bulk fluid temperatures above the critical heat flux temperature. For each hydrodynamic flow condition, one to three minuets of VHS-video filming was performed to acquire both flow regime and break-up length data. In addition to this the flow field parameters were recorded simultaneously with the filming.

1.0 INTRODUCTION

There are many diverse areas in engineering research and design in which post dryout can occur and knowledge about this phenomena is essential in order to provide accurate system analysis. Some examples include the accident analysis of PWR's such as LOCA's. In these scenarios, post dryout represents a heat transfer crisis which can lead to fuel failure. In cryogenic fluid delivery applications such as space craft and super conducting magnets it is difficult to avoid this phenomena even when "super insulators" are employed. Other examples include thermosyphons used to cool turbine blades, chemical reactors, post-accident cooling of heat generating debris, steam generators, ion-exchange columns, heat treatment in metallurgy and thermal control in VLSI electronic cooling.

A full extent, 100 cm long, flow visualization experiment was developed to examine the hydrodynamics of post dryout two-phase downflow in narrow channels at the Thermalhydraulics and Reactor Safety Laboratory (TRSL) at Purdue University [1]. The experimental investigation was divided into two parts which included a quench front propagation data series and an inverted annular break-up length data series. The quench front propagation research investigated rewetting front

speed, post dryout mechanisms during reflooding, as well as instrumentation development techniques applied to full extent visualization. These results were also compared to similar co-current upflow experiments. The inverted annular break-up length research augmented previous adiabatic work by providing data in the presence of heat transfer. In this paper, the results of the break-up length study are presented.

2.0 EXPERIMENTAL APPARATUS

The overall test apparatus is shown in figure 1. The specific components of the apparatus include: the test section, used for the hydrodynamic studies; the heat transfer system; the Freon delivery and recovery system and the gas delivery system. System variables measured are differential pressure across the test section; liquid and vapor inlet velocity; fluid subcooling (delivery temperature) and heating fluid temperature and void fraction. All system variables are obtained with fast data acquisition which is computer controlled.

The heat transfer fluid used for these experimental studies is Dow Corning's Syltherm 800, because it met essential criteria for the visualization study. First, the fluid is transparent (amber in color), it has a very low viscosity for an oil, and it is commonly used in the food technology applications since it is not hazardous if ingested and is nontoxic. The last item is important in the case of accidents, spills and vaporization of leaking fluid. The delivery system consisted of a degassing and storage tank, centrifugal delivery pump, two 8.1 kW electrical heaters and two 1.8 kW external jacket heaters, a throttle valve and assorted delivery and isolation valves and a flow meter. The system is capable of delivering the heat transfer fluid at a volumetric flow rate of 20 gpm. Constant operating temperature is monitored by a controller thermostat with an over temperature cut off. Inlet delivery temperatures were all less than ±0.5 °C during the acquisition of data. The degassing and storage tank has both gas inlet and outlets so that a nitrogen atmosphere is present during operation. This prevents the fluid from oxidizing at high temperatures.

Freon, Trichlorotrifluroethane or R-113, was the test fluid used for all of the experiments performed in this work. Freon was chosen because it is a reasonable stimulant to water, but with distinct advantages. First, it has a lower film boiling temperature and lower vapor pressure than

water, which makes the experiment easier to perform technically. Furthermore, it is one of the less reactive and hazardous of the freon class of fluids. The delivery system consists of a delivery tank, small particle fluid filter, cutoff and throttle valve, electric flow cutoff and flow meter. The recovery system consists of a dump tank, recirculation pump, and pre-cooler. Finally, the volumetric flow rate, bulk inlet and outlet temperatures and global differential pressure were measured.

For the data acquisition system a significant improvement over previous experiments of this type was provided. Primarily, this was the ability to coordinate both the video filming and the transient data obtained. This was accomplished by combining both computer controlled analog/digital data acquisition along with time display video. The need for this became apparent during some of the pre-test experiments which were performed, because a persistent oscillating phenomena was observed and it was more dynamic than reports from other vertical down flow experiments. This was amplified by the fact that during this type of oscillations, the still photography could not distinguish flow direction.

3.0 ADIABATIC EXPERIMENTAL RESULTS

3.1 Flow Regime Criteria Modifications

The purpose for this experimental series was to simulate the hydrodynamic behavior of inverted annular flow in a similar manner to previous work [2-6] and also provides an extension of De Jarlais' water studies using freon R-113. Also, the boundary condition differences between the water studies [2] and this study were investigated. And in conjunction with the boundary condition study, an evaluation of the statistical fluctuation of the time series data was also performed. Another purpose for this experimental series was to provide a "same basis" comparison of adiabatic and heat transfer data. This is essential in order to eliminate all mechanism differences except wall super heat and jet subcooling.

From an erudite point of view, the development of a flow regime criteria is some what arbitrary and qualitative, especially for visualization work. This view was expressed by De Jarlais and he noted some of the systematic problems encountered in trying to develop criteria for defining

break-up length [2]. In this work, the fundamental definitions of the four basic types of jet flow regimes are still used and include the sinuous, sinuous-varicose, varicose, and roll-wave entrainment flow regimes. However, the criteria for establishing the break-up length for these flow regimes had to be changed. The reason for this is as follows: for all flow regimes except the sinuous type, De Jarlais included wall wetting in the break-up criteria, which provided a reliable visual technique for defining break-up length, since wall wetting is easy to identify visually. This was provided as a criteria even if the interface clearly disintegrated down stream of the wall wet location.

In this work, wall wetting was ignored for this adiabatic study for two reasons. First, although wall wetting is a necessary criteria when data is acquired by direct visual or photographic observation it can be ignored in the VHS filming since many "photographs" can be acquired in a very short time relative to still-photography. Furthermore, and more importantly it is not a realistic criteria for the post dryout regime since the wall can not be wet. In addition to this, even if temporary wall contact does occur, the VHS filming technique can not distinguish it. Thus, the decision was made to ignore the wall wetting for the adiabatic case in order to allow for a consistent criteria in both the adiabatic and heat transfer studies of this work. It does, however create a minor bias between the adiabatic results in this work as compared to the previous adiabatic study.

In this study, three break-up mechanisms were observed, which are similar in characteristic to the mechanisms seen in the free jet studies and by De Jarlais' work, and they included:

Varicose Break-Up- this regime was characterized by symmetric wave on the jet core which result in alternating locations of jet expansion and contraction. When the wave form has been provided with sufficient time for the wave amplitude to reach 1/2 of the extended jet diameter then the waves forms cause droplets with diameters on the order of the most dangerous wave length.

Sinuous Break-Up- this regime was characterized by an asymmetric wave form which both distorts and displaces the liquid jet with respect to the jet's axial line of symmetry. It is distinguished by a sin-wave or snake-like shape and the mechanistic cause of this regime is the aerodynamic forces exerted by the pressure of the vapor on the liquid jet. The sinuous-

varicose break-up is a superposition of both break-up mechanisms on the jet.

Roll-Wave Entrainment Break-Up- this regime occurs at higher vapor Reynolds number flows of the sinuous break-up regime. At the crest of a sinuous wave, the decrease in pressure results in an increase in velocity until the entrainment criteria is exceeded and droplets are entrained into the vapor. In many cases this occurred very early in the flow development. In this study, similar ligament formations were seen as in previous studies; however, the droplet formations which have been observed using still photography could not be observed with the VHS filming because of the slow filming rate.

3.2 Analysis of Break-up Length

For the adiabatic series, the exit pressure boundary was not open to the atmosphere, and all of the data for the test matrix was acquired, analyzed and extensively compared to the open boundary work [2]. Analysis of the break-up data included investigating: (a) the error analysis of the filming method; (b) comparisons of time series break-up length data; (c) comparisons of initial disturbance data; (d) the break-up lengths dependence on gas velocity; (e) pressure fluctuation data; (f) velocity fluctuation analysis.

From the literature it was apparent that there exists concern over the break-up length fluctuation and the ability to quantify the actual mean deviation of data [2,7-10]; however, this is not usually done because in the past it has been prohibitively expensive and excessively time consuming. In view of this problem, and in light of the (relative) ease that the VHS filming can be performed, an error analysis was performed similar to the statistical method used by Wilmarth [11]. In this method, the long term mean fluctuation was examined (via numerical simulation) as a function of sample size in order to determine how large a sample space was required in order to obtain a convergent mean value.

Wilmarth's work was extended in order to provide a more rigorous convergence criteria and was then applied to the jet break-up data acquired for this research. For the jet data both a "stable" or convergent mean value and a "stable" or convergent sample-deviation were necessary so that

reliable plots of these quantities could be provided. The rational for such a criteria can be justified by application of the law of large number. Although both the mean:

$$\bar{X} = \frac{1}{N}\sum_{i=1}^{N} X_i \quad , \tag{1}$$

And the absolute mean deviation of the sample space:

$$s_{M.D.} = \frac{1}{N}\sum_{i=1}^{N} |X_i - \bar{X}| \quad , \tag{2}$$

are guaranteed to converge to the actual values as $N \to \infty$, the convergence rates are not necessarily the same. Thus, the convergence rate of both quantities must be investigated in order to determine which rate is the most restrictive in term quantifying the minimum sample space needed. A typical example of the sequence of events for this type of analysis are provide in figures 2 to 4. For the break-up length data of time series F7.1, both the mean and deviation are plotted as a function of sample space size. From the figures two typical trends were noted. First, the mean value in this example (and for virtually all the data sets) usually converged prior to the variance, and so the stability of the absolute mean deviation became the restrictive criteria for the minimum sample space instead of the mean value used in Wilmarth's research. Secondly, the mean value almost always converged by 30 samples, indicating that when only mean value information is necessary, the VHS filming method is far superior to the still photography method by virtue of the smaller sample size and by virtue of the much faster data acquisition and reduction time.

The investigation of a minimum sample space criteria was also conducted as a function of gas velocity. A plot of break-up lengths for an extended range of gas velocities is provided in figure 5 along with the mean and absolute deviation calculations provided in figures 6 and 7 respectively. Surprisingly, even though the instantaneous fluctuation of the data seems to be qualitatively different as gas velocity increases, the convergence of the mean seem to be relatively independent of velocity. Again, the absolute mean deviation seems to control the minimum sample space criteria, which was determined to be $N \geq 60$.

With the sample space criteria firmly established, then both the stable mean and standard deviation of the jet break-up data were plotted as a function of inlet gas velocity. A typical set of jet break-up length data for the freon R-113 jet is shown in figure 8. These results indicate that at low gas velocities, V_g, (within the standard error of the experiment) a relatively constant value of break-up length results. But at some point, once the aerodynamic influences of the gas become important, then the break-up length monotonically decreases as gas velocity increases. Furthermore, as the break-up length decreases, the standard error decreases. This indicates a more vigorous and stable disturbance on the vapor-jet interface. This can be justified on a semi-quantitative basis by examining the initial disturbance written in Fourier series form:

$$\delta(z,t) = \delta_0 \exp(\alpha t + kz) \quad , \tag{3}$$

where δ is the initial disturbance, α is the growth rate of the disturbance, k is the wave number and z is the position of the disturbance. As the turbulence amplitude and frequency increases at some fixed position, say the jet outlet, then the break-up length will occur in a shorter distance. Furthermore, as the wave number increases so does the frequency which also decreases the break-up length. The smaller standard error can be accounted for by considering both the frequency spectrum of a turbulent flow and the aerodynamic forces. Klebanoff [12,13] and Kovaznay et. al. [14] have investigated the turbulence phenomena. Their results indicate that near an interface, such as the liquid vapor interface at the vapor jet injection site, the frequency of the turbulence eddies increase and the spectral variation decreases. This would result in a smaller variation in the jet break-up length. Also, as the vapor velocity increases, the pressure gradient and interfacial shear act against the cohesion influence of surface tension, which results in an earlier break-up of the jet.

The adiabatic data of this study was also extensively compared to the adiabatic work of De Jarlais. A direct comparison of similar jet velocity data under similar experimental conditions are presented in figure 9. When plotted to scale, it becomes immediately evident that both the overall magnitude of the break-up length and the general trend of the data compare very well to De Jarlais data, although for the data of this thesis the break-up length seems to decrease some what faster at the high end of the velocity abscissa. This curve also shows that the overall break-up mechanisms of the free jet and confined jet works are consistent over variation in gas velocity, gas density, liquid

density and Ohnesorge number. From the figure it is obvious that two mechanisms exist and that the a clear transition takes place on the order of 2-3 m/s since the power of velocity dependence changes from zero to about one. Furthermore, the liquid velocity dependence can be clearly seen in the gas independent region since the breakup length increases with liquid velocity.

One systematic difference between this adiabatic study and the previous study [2] is in the global pressure response. When the exit pressure boundary remained open to the atmosphere, the magnitude of a typical pressure reading was considerably lower than the results obtained in this research. Furthermore, the fluctuation of De Jarlais' data was less than 1/10 the average value of the current study. In figure 10 the differential pressure data for two extreme gas flow velocities is plotted. From the figure three important points can be made. First, the overall magnitude of the pressure reading for this study was a factor of 5 to 7 greater than the pressure reading of the previous study. Also, for the closed boundary experiment, the magnitude of the differential pressure changed by 25% over the range of velocities investigated in the study. Finally, the pressure fluctuation of this study became both intermittent and larger as the gas velocity increased.

This pressure fluctuation affect is particularly difficult to analyze since it is both stochastic and global. The combined problems of the fluctuation being both intermittent and stochastic makes it unlikely that a deterministic representation of the pressure field can be realized. The reason for this is run time. In order to characterize both the amplitude and burst frequency, very long run times would be necessary; however, these long run times are prohibited due to the loss of freon involved. The results of the data available can be qualitatively used to explain the small increase in break-up length for the high velocity data relative to the open boundary study. Initially, the fluctuation of the pressure field can be viewed as an equivalent fluctuation in the velocity field by making an approximate Bernoulli analysis. This is done by assuming that the inertia of the liquid jet is much greater than the gas core and then neglecting any compressibility affects on the gas density. This allows the pressure field to be written as:

$$\Delta P_{dif} \doteq 1/2\, \rho_G \Delta V_G^2 \quad , \tag{4}$$

where the gas density is on the order of one. Thus, the influence of pressure fluctuation could be

converted to a velocity fluctuation which is on the order of 5 to 10 %. This increased fluctuation in the interfacial shear would tend to slightly enhance the break-up of the jet.

3.3 Mechanistic Model Development

From the data in figure 9 it was apparent that the data could be separated into two distinct regions. The first, was a constant gas velocity region which had a jet velocity dependence. The second was a gas velocity dependent region.

In the first region, the free jet data results can be used to qualify scaling criteria, since the results are fairly similar. The results of Weber, Middleman and others [15-18] show that the jet break-up has a functional form:

$$\frac{L_B}{D_j} \propto Re_j^N \sqrt{We_j} \quad . \tag{5}$$

This form assumed a varicose and laminar jet and relinquishes the surface disturbance term to a fitting coefficient. This, is a reasonable procedure from an experimental point of view, since it is nearly impossible to accurately measure the initial disturbance, let alone provide a relationship between it and the jet break-up length. The correlation form could also be written in terms of a modified capillary number similar to Ishii and Denten [19].

For the region where the gas core begins to induce an aerodynamic influence a drag relation similar to the inception criteria for film flow can be applied in analogy [20-21]. For the jet, it is assumed that beyond some criteria point the drag force on the jet interface becomes significant, thus, the drag force acting on the perturbed region of the jet would be proportional to the relative velocity:

$$F_d \propto \rho_G V_{G,rel}^2 \quad . \tag{6}$$

Also, as the liquid jet increases in diameter, for a fixed confinement diameter, the interfacial shear term is modified by virtue of the velocity profile modification which occurs. Thus there is a diameter

ration influence which must be accounted for. Since the diameter ratio is related to the void fraction, this is the variable of choice. Again, from the free jet data, where the drag induced asymmetric waves occurred, most correlations appear in the form of a relative gas Weber number. These two influences were combined in to one term which included both the drag and the void fraction affects. This resulted in the formulation:

$$\frac{L_B}{D_j} \propto (We_{G,rel} / \alpha^2)^M \quad , \tag{7}$$

and would be applicable beyond the transition criteria. The data of this study was examined for the transition criteria based on a relative gas Weber number and it was determined that:

$$We_{G,rel} / \alpha^2 = 1.63 \quad , \tag{8}$$

which was very close to the criterion developed by Iciek [9,10].

With this in mind, it was decided to evaluate the data of this work against the previous adiabatic data in order to determine how closely the data correlated. In Figure 11 the adiabatic data was plotted for the liquid jet modified break-up length as a function of the modified gas Weber number. Essentially, there is good agreement between the results. Two observation should be noted. First, the data seem to be slightly high as compared to De Jarlais' results however the results are still within the standard error of his data. Furthermore, at extremely high velocities, the break-up length of this work begins to decrease at a faster rate. This phenomena would be worth examining as a continuation study at a future date; however it would be more appropriate to use a closed boundary water system because the current experimental apparatus can not afford the freon loss associated with high gas Weber number flow.

4.0 DIABATIC RESULTS

4.1 Experimental Test Matrix

The purpose of the diabatic experimental series was to simulate hydrodynamic behavior coupled with liquid and wall boundary thermodynamic influences. This represents experimental work which has not previously been acquired, and this work provides an additional extension to both the water studies and the results of section 6.1. Furthermore, this work also provides a resource for comparison between the upflow results of Ishii and Co-workers [22-27].

The overall filming procedure for the adiabatic experiments was not acceptable for much of the diabatic experimental series. This was due to an optical problem. During filming, the maximum range of the test section that could be visualized and the break-up interface clearly identified was 25 cm. Thus, four viewing regions were necessary in order to acquire data from the full extent of the test section 100 cm long. Now for all of the adiabatic data, the maximum deviation of the break-up data never exceeded 15 cm; however, for the diabatic data series, maximum deviation could be as high as 35 cm. For these cases a fundamental problem existed in terms of the data acquisition: how does one accurately determine the mean value of the time series when all of the time series is not captured by the viewing region? An example of the data series acquired from the H68 test is presented in figure 12.

This problem of determining the actual break-up length is additionally aggravated by the fact that it is possible for the jet to simultaneously break-up in multiple location. Hence, it can be unclear if a the break-up viewed in a lower viewing window (such as the 45-70 cm view of figure 12) is truly the first break-up location or if it is one of the multiple locations which occurred in the upper viewing window (which is the 60-85 cm view of figure 12). Mathematically, this is a problem of statistical inference when one of the dependent variables is a function of the another dependent variable. This can be seen by considering the data of figure 12. Let the break-up data of the 60-85 cm view be referred to as L_{B1} (t) and the break-up data of the 45-70 cm view be referred to as L_{B2} (L_{B1} (t) , t). This means that the probability of an event (eg. the break-up length) in the lower view field is conditional based on the weather the break-up occurred in the upper view field. Physically,

what we want to do is subtract out the dependence of L_{B2} on L_{B1}. However, the experimental problem with doing this task is that we do not know how often (eg. the frequency) this event occurs. Thus, we are forced to make a formal guess as to the frequency of the event even though we have no experimental basis for the formulation. Essentially, the only way to obtain this information is to simultaneously film both regions and determine the frequency in which multiply viewed break-up's occur.

In this research the total probability of the jet break-up occurring in both view windows is:

$$P(L_{B,total}) = P(L_{B1}) + P(L_{B2}) - P(L_{B1} \bigcap L_{B2}) \quad , \tag{9}$$

where $L_{B,total}$ is the total break-up events which occur. This can be put into a sample space estimate of the mean value for $L_{B,total}$ by assuming that the break-up events in each window are mutually exclusive. Thus, the mean value can be written:

$$\overline{L}_{B,total} = f_1 \overline{L}_{B1} + f_2 \overline{L}_{B2} - f_1 f_2 \overline{L}_{B1} \quad , \tag{10}$$

where f represents the sample frequency of the view field.

4.2 Analysis of Diabatic Break-up Length

For the diabatic series, all of the data for the test matrix was acquired, analyzed and extensively compared to the previous adiabatic research [2-6], the previous diabatic up-flow research[22-27] and the current adiabatic research. Analysis of the diabatic break-up length included: (a) the error analysis of the filming method; (b) the pressure fluctuation influence; (c) the flow field error analysis; (d) the comparison of diabatic and adiabatic data and; (e) comparison to the up-flow data.

Within the literature examined to date, the actual break-up length fluctuation of diabatic data has never been a statistical evaluated, and so one of the tasks of this research was to develop a methodology and sample space criteria similar to the results developed for the adiabatic data. In section 6.1.3 it was experimentally determined that the criteria for the adiabatic data acquisition was:

$$N \geq 60 \quad , \tag{11}$$

where N is the size of the sample space. In the case of the diabatic data, as shown in figure 12, it is possible to collect fewer "hits" in the sample space since the sample frequency is less than one. And the only true measure of the statistical convergence is the convergence of the actual break-up events visualized. Furthermore, from equation 11 it is necessary that the total break-up length converge. This can only be assured by guaranteeing that the data series is piece wise convergent for each individual viewing range. In view of this, one can modify the adiabatic criteria of equation 12 to be:

$$f_k N_k \geq 60 \quad , \tag{12}$$

where f is the sample frequency of the viewing window and N is the total size of the sample space. The index k = 1 or 2, refers to the first of second viewing range respectively. This sampling criteria forced the size of the filming sample space to be on the order of 120 to 240 samples (at 1/30 sec per sample) for most of the diabatic data obtained in this work. The application of this criteria unfortunately increased by as much as a factor of four the amount of raw data necessary to develop each data point; however, even at this significant increase in raw data acquisition, this technique is still faster and more reliable than the still photography method.

For the adiabatic data the pressure response was determined to be the cause for decreasing the break-up length as the modified gas Weber number, $We_{g,rel}$, increases beyond the roll wave criteria; however due to the intermittent nature of the fluctuation, the influence was measurable but small. This phenomena drastically changes for the diabatic data which is shown in figure 13. For the diabatic data two consistent trends were observed. First, the pressure fluctuation is strongly dependent on both the inlet liquid flux and subcooling:

$$\Delta P_{diff} = \Delta P_{diff}(J_L, \Delta T_{sub}) \quad . \tag{13}$$

As the liquid flux increased at a fixed subcooling, both the magnitude of the pressure signal and the magnitude of the pressure fluctuation increased. Physically, this is due to the increased vaporization of the freon in the heated channel: this mechanism is non-intuitive, since it is the opposite of what happens in pre-CHF flows. In inverted annular flow, the liquid jet is insulated from the wall heat

transfer by the vapor blanket until after break-up occurs. After break-up occurs, then entrainment and deposition rates govern the wall impingement which causes vaporization. Thus, as the jet velocity increases the jet break-up length decreases and this effectively provides a longer path for droplet impingement to occur. Subcooling has less of an influence on the net vaporization; however, it does control re-condensation of the vapor which can result in large pressure variations. Figures 10 and 6.13 can be compared in order to show the order of magnitude difference between the adiabatic and diabatic situations.

In the case of the low liquid flux high, subcooling diabatic flow the pressure signal is similar in magnitude and pressure fluctuation to the adiabatic case and thus the axial extent should be about the same order of magnitude. As the pressure fluctuation increases the results should be to increase the relative velocity (and it's fluctuation) at the interface. This increase in interfacial shear will cause the jet to disintegrate sooner which should decrease the break-up length. Furthermore, the more violent global perturbation on the jet inter face will also provide for a broader spectrum of the initial disturbances which will increase the deviation of the break-up fluctuation. The pressure fluctuations for the diabatic data can be nearly 100% in the high liquid flux and low subcooling cases. For the system pressure instrumentation, the validine pressure transducer was only rated for ± 5 Psid, and so it can be seen from the figure that the pressure well exceeded the diaphragm limitation an could potentially damage the device. Furthermore, the instantaneous pressure fluctuations can be estimated to be on the order of 40 psi static equivalent. Since the test section is only rated for 50 psi, this violent pressure swing represented a potential safety problem. Thus, the low subcooling tests were restricted.

The results of the flow field error analysis is presented in figure 14. Here we can draw three conclusions about the diabatic data. First, the qualitative discussion concerning the pressure fluctuation is representative of the actual data. Thus the decrease in the subcooling results in a decrease in diabatic break-up length. Next, the standard error of the break-up length increases as the subcooling decreases. This can be interpreted from the pressure fluctuation analysis and is due to the increased perturbation of the liquid interface. The increase in the error in the Reynolds number is also due to the pressure fluctuation. From the data, as the subcooling decreased and the pressure fluctuation increased, the back pressure in the test section resulted in changing the liquid jet velocity

as much as 50%. This results in a proportional degradation of the jet Reynolds number uncertainty. It must be noted that in this case the uncertainty is caused by the phenomena and is not a error in the conventional instrumentation sense.

The jet break-up length was also compared to the adiabatic correlation, and those results are shown in figure 15. Here the dimensionless break-up length modified by the liquid jet parameters is plotted as a function of modified Weber number. Although the functional form seems to be correct, the subcooling is an influence which must be accounted for in order to reduce the data into a single line an be dimensionless. From these results it is also apparent that the adiabatic correlation is fairly accurate for much of the subcooling range. But as the pressure influence increases the mechanism is not accounted for by the present theory.

These results have also been compared to the up-flow data of Ishii and co-workers. In this research, it was noted that the quotient of the jet Weber and Reynolds is equivalent to the Capillary number and so the data was formulated as a function of that parameter. An example of these results are provided in figure 16. With some manipulation it can be shown that the jet break-up for the upflow is less than 1/10 the axial extent of the concurrent downflow. The results are even more severe when the data of this research is compared to the data of Babelli. Currently, within the literature there is no theoretical explanation to account for the difference between these flow situations.

4.3 Diabatic Dimensionless Break-up Length Results

The methodology applied to the development of a dimensionless break-up length was to build on the mechanistic model of Ishii, De Jarlais and Co-workers [2-6,20-27], and then to provide an extension of the adiabatic results for the post dryout diabatic flow fields. The principle reasoning for this is that the overall response of the heat transfer data shown in figure 15 is qualitatively similar to the adiabatic data however there is also a clear thermodynamic affect which decreases the break-up length. This result has not currently been quantified in the literature.

The order of magnitude of the subcooling affect can be more clearly quantified by observing the raw data of break-up length as a dependent variable of the subcooling as an independent variable.

This is shown in figure 17. This shows a proportionality which is approximately second order:

$$L_B \propto \Delta T_{sub}^2 \quad . \tag{14}$$

Furthermore, if a formal regression analysis of the raw data, as shown by the dotted line, is performed then the power is quantified as 2.03. In addition to this, the overall fit of the data to the regression analysis is R = 90, which nominally adequate. The one shortcoming of this result is that while it is clearly a natural variable for developing a dimensionless result it precludes us from developing an encompassing model for both the adiabatic and diabatic data simultaneously. However, if the result is framed in the context of an actual reactor problem, the this is acceptable since inverted annular flow can not exist in a truly adiabatic flow field.

In order to provide a mechanistic development of the thermodynamic influence in terms of a dimensionless property of the flow field we note that the vaporization seems to be the dominant factor involved in decreasing the break-up length. Thus, it is postulated or assumed that a dimensionless break-up length should be a function of the hydrodynamic or momentum influences as provided by the adiabatic study and a yet undetermined thermodynamic influence, T^*:

$$L_B^* = L_B^*(Re_j, We_j, We_{G,rel}^*, T^*) \quad , \tag{15}$$

where L* is the dimensionless break-up length, Re and We are the Reynolds and Weber numbers respectively with the subscript j indicating a jet property, and $We^*_{G,rel}$ is the void fraction modified gas Weber number. Next, it is also assumed that the principle mechanisms are due to subcooling and due to heat transfer available for vaporization. This implies that there would be a heat transfer influence on the order of the temperature difference between the wall and the fluid. Thus we would write the dimensionless variable as a ratio of these two affects. Furthermore, we require them to be functionally correct with respect to the results of figure 17. First, we require the break-up length to decrease as the subcooling approaches zero, or $L^* \to 0$ as $T^* \to 0$. Furthermore, as heat transfer to the liquid increases the break-up length must again approach zero. This requires the affect to be inversely proportional to the break-up length. Thus were formally assume the dimensionless form:

$$T^{*} = \frac{T_{sat} - T_F}{T_{wall} - T_{sat}} \quad , \tag{16}$$

where T_{sat} is the saturation temperature of the fluid, T_{wall} is the system wall temperature and T_f is the fluid temperature. This form of dimensionless or normalized temperature meets the physical restrictions determined from the diabatic data.

By constructing a correlation form, from equations 16 and 17, we obtain the general functional form:

$$L_B^{*} = K(Re_j)^m (We_j)^n (We_{G,rel}^{*})^p (T^{*})^q \quad , \tag{17}$$

where L^{*}_B is the break-up length normalized by the jet diameter; K is the fitting coefficient; Re_j, We_j are the jet Reynolds and Weber numbers respectively; and $We^{*}_{G,rel}$ is the void fraction normalized gas Weber number. Also, m, n, p, q are power coefficients which must be determined experimentally. In order to simplify this correlative process it is noted that the functional change of the momentum processes seems to be similar to the adiabatic data. Thus, we assume the coefficients m, n and p as developed in De Jarlais work. Furthermore, we can then develop values for K and q from the diabatic data directly by applying regression analysis techniques. When this is done, the value of K is 3.0e5 and the value of q is 2.029. Thus we can write the final form of the dimensionless axial extent or break-up length as:

$$L_B^{*} = 30000(Re_j)^{-0.53}(We_j)^{0.5}(We_{G,rel}^{*})^{-0.645}(T^{*})^{2.029} \quad . \tag{18}$$

The correlation was applied to the diabatic data series and was plotted as a function of the fluid variables versus the gas variables. This result is shown in figure 18. From the figure it can be seen that the data reduces fairly well. However, a restrictions is implicit in the correlation because of the difficulty in changing the liquid subcooling. Thus, caution should be observed in applying the correlation beyond the reliable subcooling range of the data base which is $5\ C \leq \Delta T_{sub} \leq 35\ C$.

5.0 CONCLUSIONS

For the adiabatic series, the work of Ishii and Co-workers was extended in several significant ways. First, accurate void fraction data acquisition was provided along with the determination of break-up length, and this was performed for the closed atmosphere exit boundary condition. In addition to this, complete time series data acquisition of the flow field variables were obtained. The influence of pressure fluctuation on the break-up length for high flow rates was observed, analyzed and was shown to decrease the break-up length. Furthermore, the data results were examined on a mechanistic level and the results obtained in this work were shown to be in good agreement with the previous results of De Jarlais.

For the heat transfer series, this work represents the only post dryout visualization study for concurrent downflow with heat transfer. The results provide a mechanistic means for evaluating heat transfer influences on the break-up length as a function of fluid subcooling. The most significant problems for the diabatic break-up length are the global system changes, such as pressure fluctuation, on the local perturbations which cause instabilities. This results in a modification of the break-up length which causes transition from inverted annular to inverted slug flow sooner than predicted by previous studies.

The break-up length fluctuation series represents the only instantaneous time fluctuation data ever acquired for the confined jet problem. This work provides an accurate statistical evaluation of the break-up length, and it also provides an accurate evaluations of the break-up frequency and flow regimes of the jet. Furthermore, it should be noted that this method makes the entire process of data acquisition and analysis much faster, cheaper and more accurate than the photographic method.

6.0 REFERENCES

[1]. C. S. Eberle, "Experimental and Theoretical Considerations Concerning the Hydrodynamics of Post Dryout in Two-Phase Downflow," Ph.D. Thesis, Purdue University, 1994.

[2]. G. De Jarlais, "An Experimental Study of Inverted Annular Flow Hydrodynamics Utilizing an Adiabatic Simulation," Argonne National Laboratory Report, ANL-83-44, NUREG/CR-3339, 1983.

[3]. G. De Jarlais and M. Ishii, "Hydrodynamics of Adiabatic Inverted Annular Flow - An Experimental Study," 3rd Multi-Phase Flow and Heat Transfer Symposium, Miami Beach, FL, Vol. 1, 317-331, 1984.

[4]. G. De Jarlais, M. Ishii and J. Linehan "Hydrodynamic Stability of Inverted Annular Flow in an Adiabatic Simulation," ASME J. Heat Transfer 108, 84-92, 1986.

[5]. G. De Jarlais and M. Ishii "Inverted Annular Flow Experimental Study," Argonne National Laboratory Report, ANL-85-31, NUREG/CR-4277, 1985.

[6]. M. Ishii and G. De Jarlais "Flow Regime Transition and Interfacial Characteristics of Inverted Annular Flow," Nucl. Eng. Des. 95, 171-184, 1986.

[7]. R.M. Christiansen and A.N. Hixson, "Break-up Length of a Liquid Jet in a Denser liquid," Ind. Eng. Chem. 49, pg. 1017, (1957).

[8]. T.F. Chen and J.R. Davis, "Disintegration of a Turbulent Water Jet," Proc. ASCE, Hyd. Div. 90, Pg. 175, (1964).

[9]. J. Iciek, "The Hydrodynamics of a Free, Liquid Jet and their Influence on Direct Contact Heat Transfer -I," Int. J. Multiphase Flow 8, 239-249, 1982.

[10]. J. Iciek, "The Hydrodynamics of a Free, Liquid Jet and their Influence on Direct Contact Heat Transfer -II," Int. J. Multiphase Flow 8, 251-260, 1982.

[11]. T. L. Wilmarth, "A Study of Two-Phase Flow Characteristics in Narrow Channels," MSNE Thesis, Purdue University, (1993).

[12]. P.S. Klebanoff, "Characteristics of Turbulence in a Boundary Layer with Zero Pressure Gradient," NACA Report No. 1247, (1955).

[13]. P.S. Klebanoff, K.D. Tidstrom, "Mechanisms by Which a Two-Dimensional Roughness Element Induces Boundary Layer Transition," Phys. Fluids 15, 1173-1188, (1972).

[14]. L.S.G. Kovaznay, V. Kibens and R.F. Blackwelder, "Large Scale Motion in the Intermittent Region of a Turbulent Boundary Layer," J. Fluid Mech. 41, 283-325, (1970).

[15]. R.P. Grant and S. Middleman, "Newtonian Jet Stability," A.I.Ch.E Journal 12, 669-678, 1966.

[16]. R.W. Fenn and S Middleman, "Newtonian Jet Stability: The Role of Air Resistance," A.I.Ch.E Journal 15, 379-383, 1969.

[17]. R.E. Phinney, "Stability of a Laminar Viscous Jet - The Influence of the Initial Disturbance Level," A.I.Ch.E Journal 18, 432-434, 1972.

[18]. R.E. Phinney, "Break-up of a Turbulent Liquid Jet in a Low-Pressure Atmosphere," A.I.Ch.E Journal 21, 996-999, 1975.

[19]. M. Ishii and J.P. Denten, "Flow Regime Transition and Interfacial Characteristics of Inverted Annular Flow," Nucl. Eng. Des. 99, 171-184, (1986).

[20]. M. Ishii and M.A. Grolmes, "Inception Criteria for Droplet Entrainment in Two-Phase Concurrent Film Flow," A.I.Ch.E. Journal 21, 308-318, 1975.

[21]. G. Hestroni Ed., "Handbook of Multi-Phase Flow," Hemisphere Pub, 1983.

[22]. N.T. Obot and M. Ishii, "Two-Phase Flow Regime Transition Criteria in Post-Dryout Region Based on Flow Visualization Experiments," Argonne National Laboratory Report, ANL-87-27, NUREG/CR-4972, 1987.

[23]. N. T. Obot and M. Ishii, "Two-Phase Flow Regime Transition criteria in Post-Dryout Region Based on flow Visualization Experiments," Int. J. Heat Mass Transfer 31, 2559-2570, 1988

[24]. J.G. Denten and M. Ishii, "Flow Visualization Study of Post Critical Heat Flux Region for Inverted Bubbly, Slug, and Annular Flow Regimes," Argonne National Laboratory Report, ANL-88-27, NUREG/CR-5171, 1988.

[25]. M. Ishii and J.P. Denten ,"Two-Phase Characteristic of Inverted Bubbly, Slug and Annular Flow in Post-Critical Heat Flux Region," Nucl. Eng. Des. 121, 349-366, 1990.

[26]. I.M.M. Babelli, "Flow Visualization Study of Post-Critical Heat Flux in Inverted Flow," M.S Thesis, Purdue University, 1992.

[27]. I.M.M. Babelli, S.T. Revankar and M. Ishii, "Flow Visualization Study of Post-Critical Heat Flux in Inverted Flow," Nucl. Eng. Des. 146, 15-24, 1994.

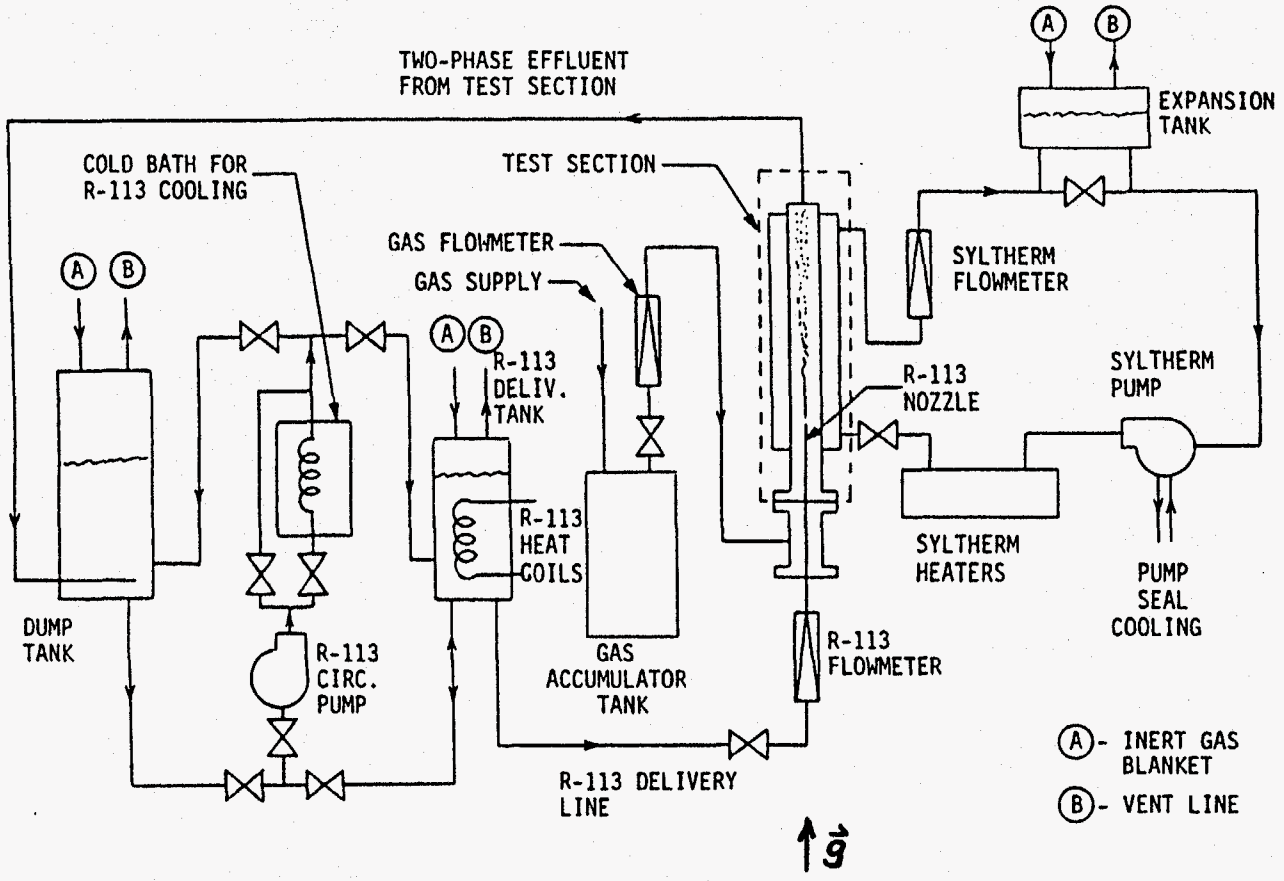

Figure 1. Schematic of overall test apparatus.

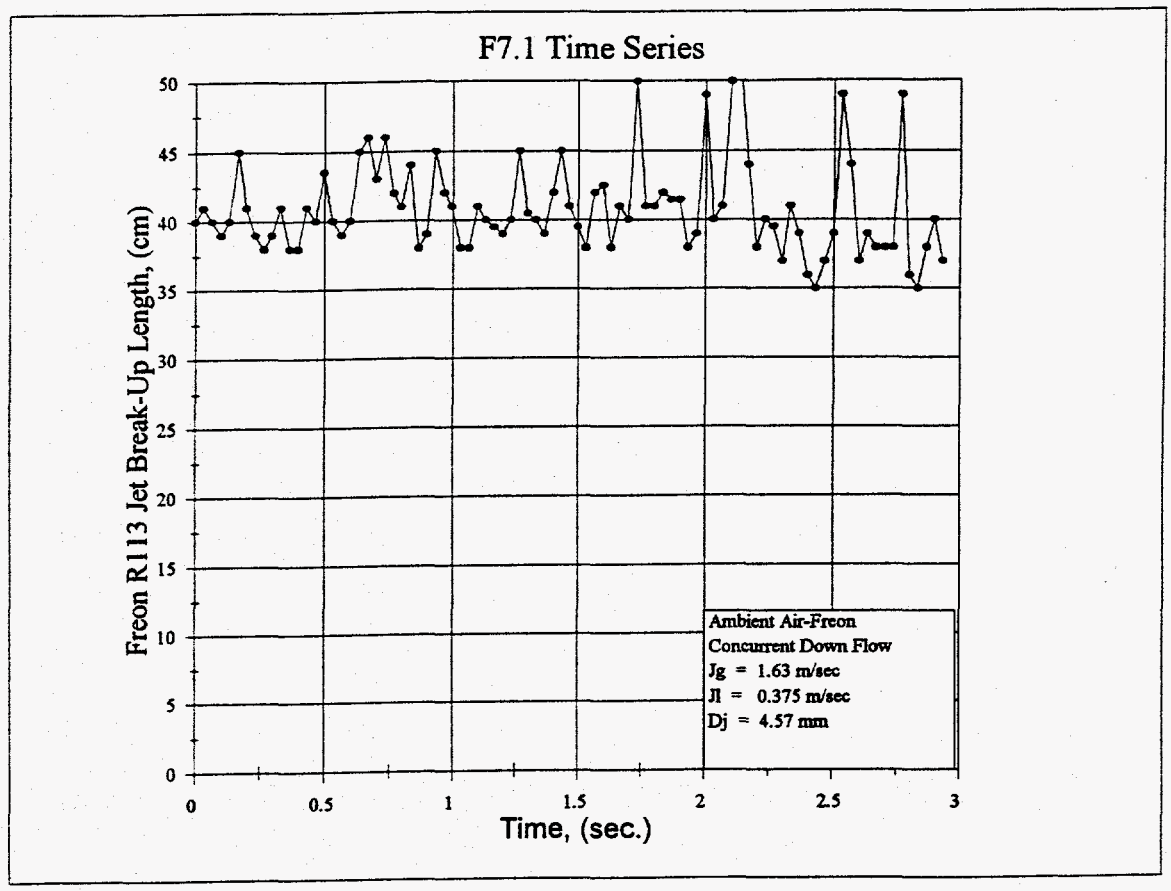

Figure 2. Break-up length data for time series F7.1.

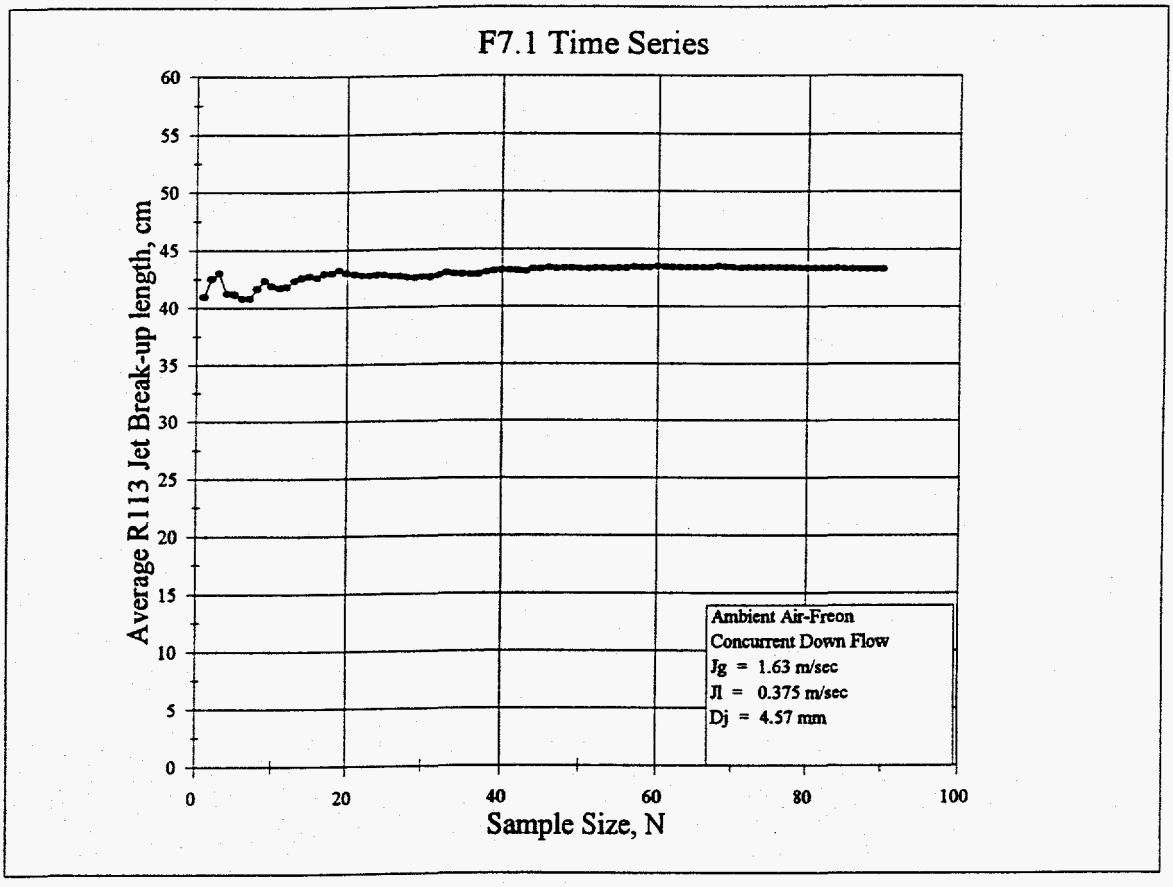

Figure 3. Average break-up length versus sample size for F7.1 data.

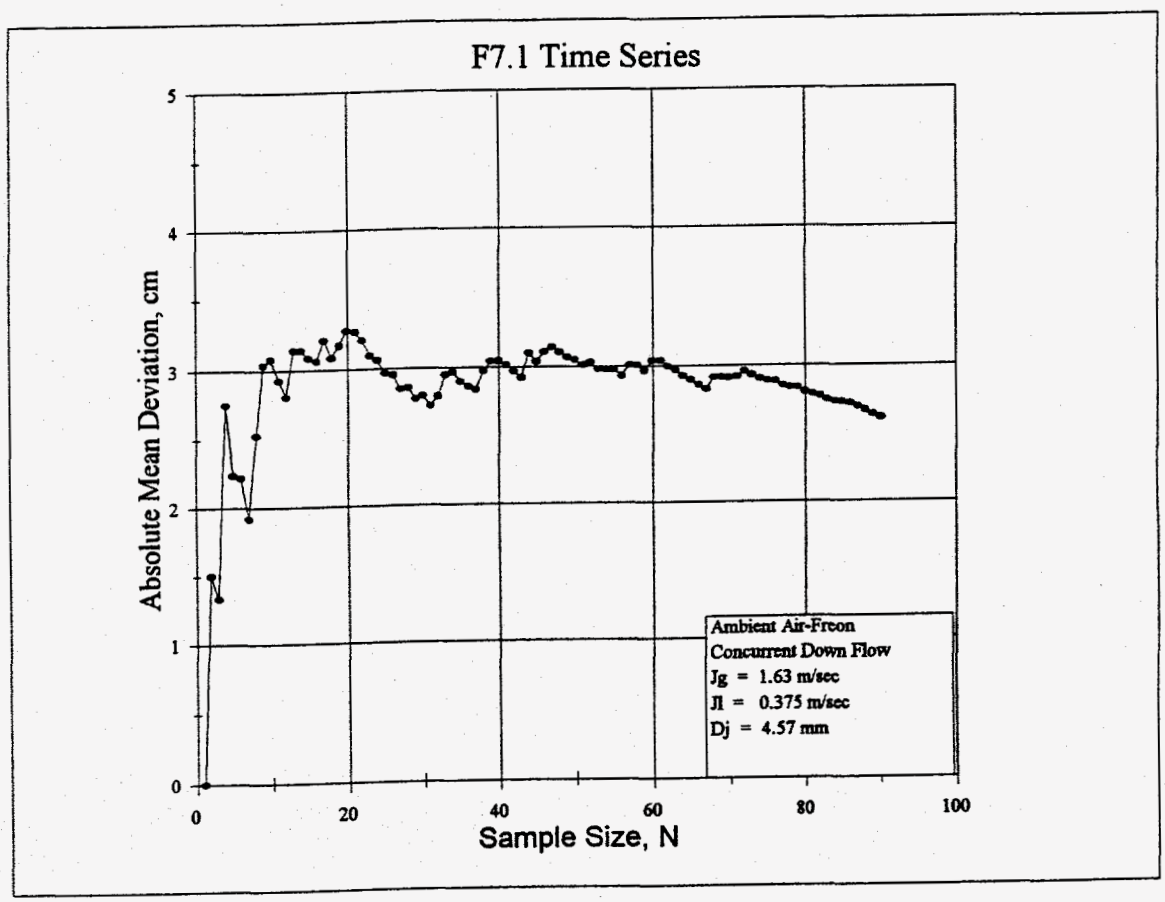

Figure 4. Absolute mean deviation of F7.1 data.

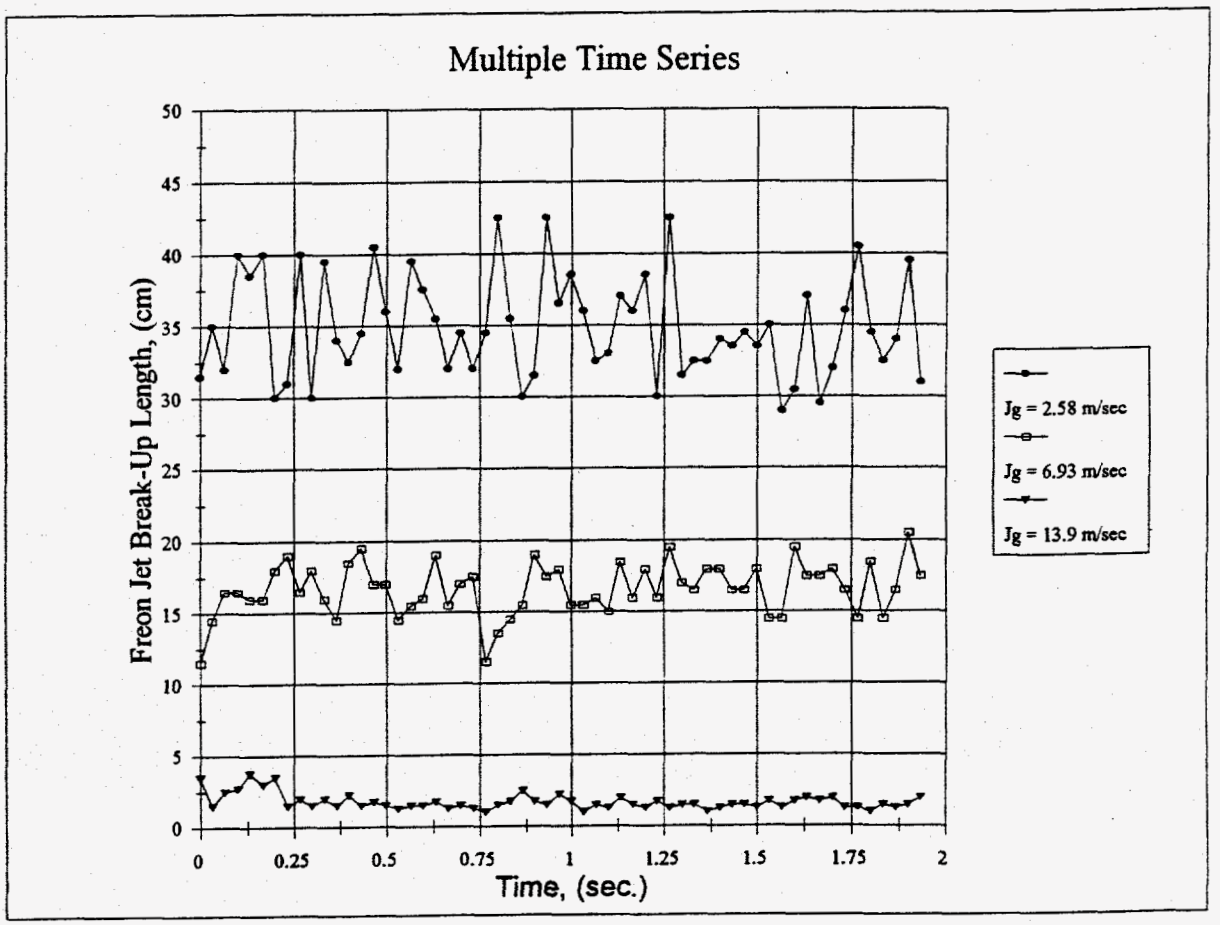

Figure 5. Comparison of break-up data for various gas velocities.

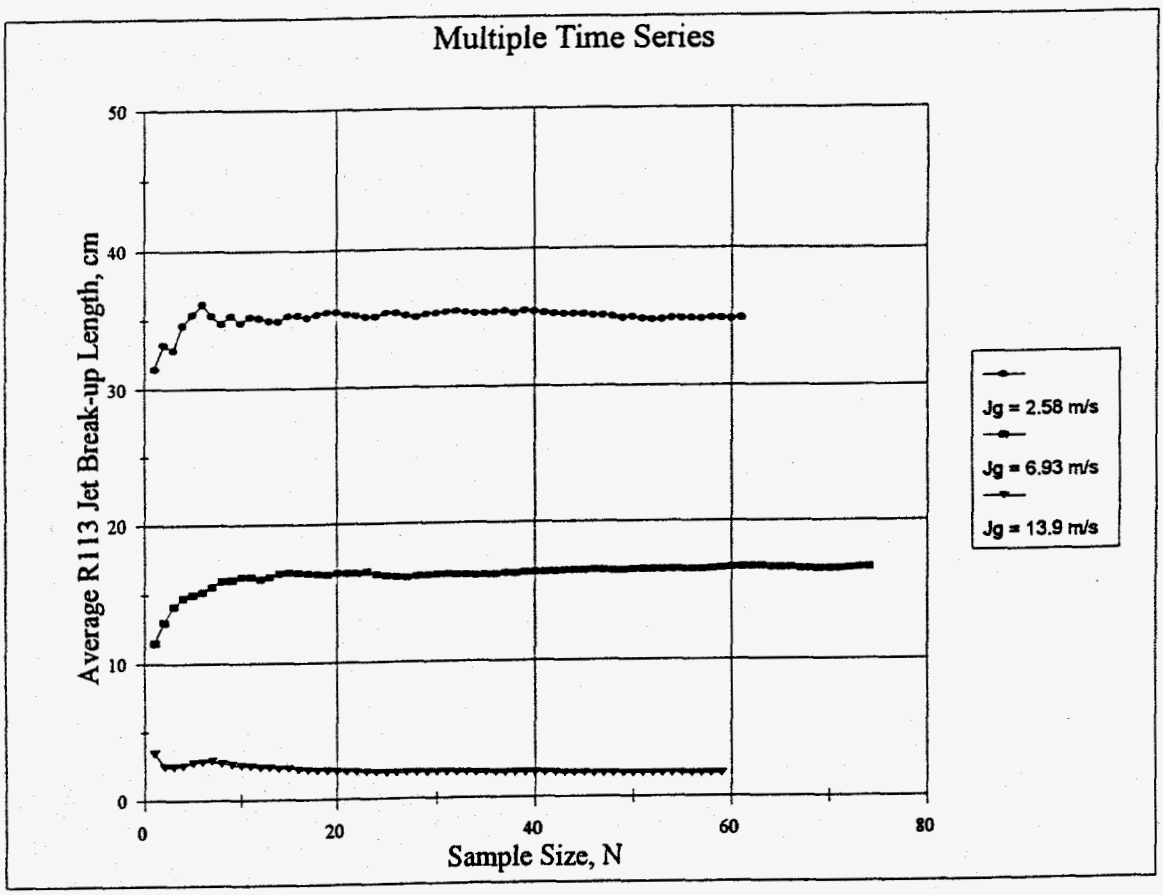

Figure 6. Comparison of average break-up data for various gas velocities.

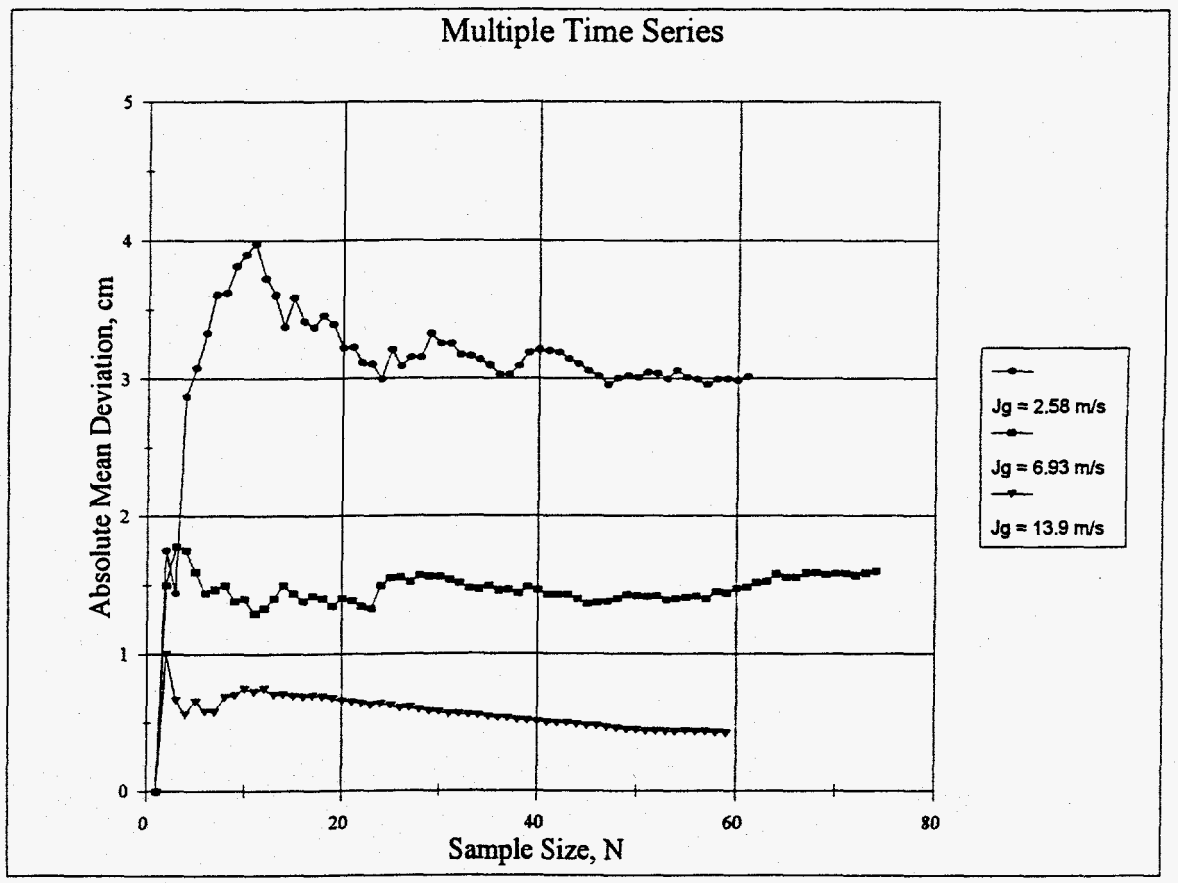

Figure 7. Comparison of absolute mean deviations for various gas velocities.

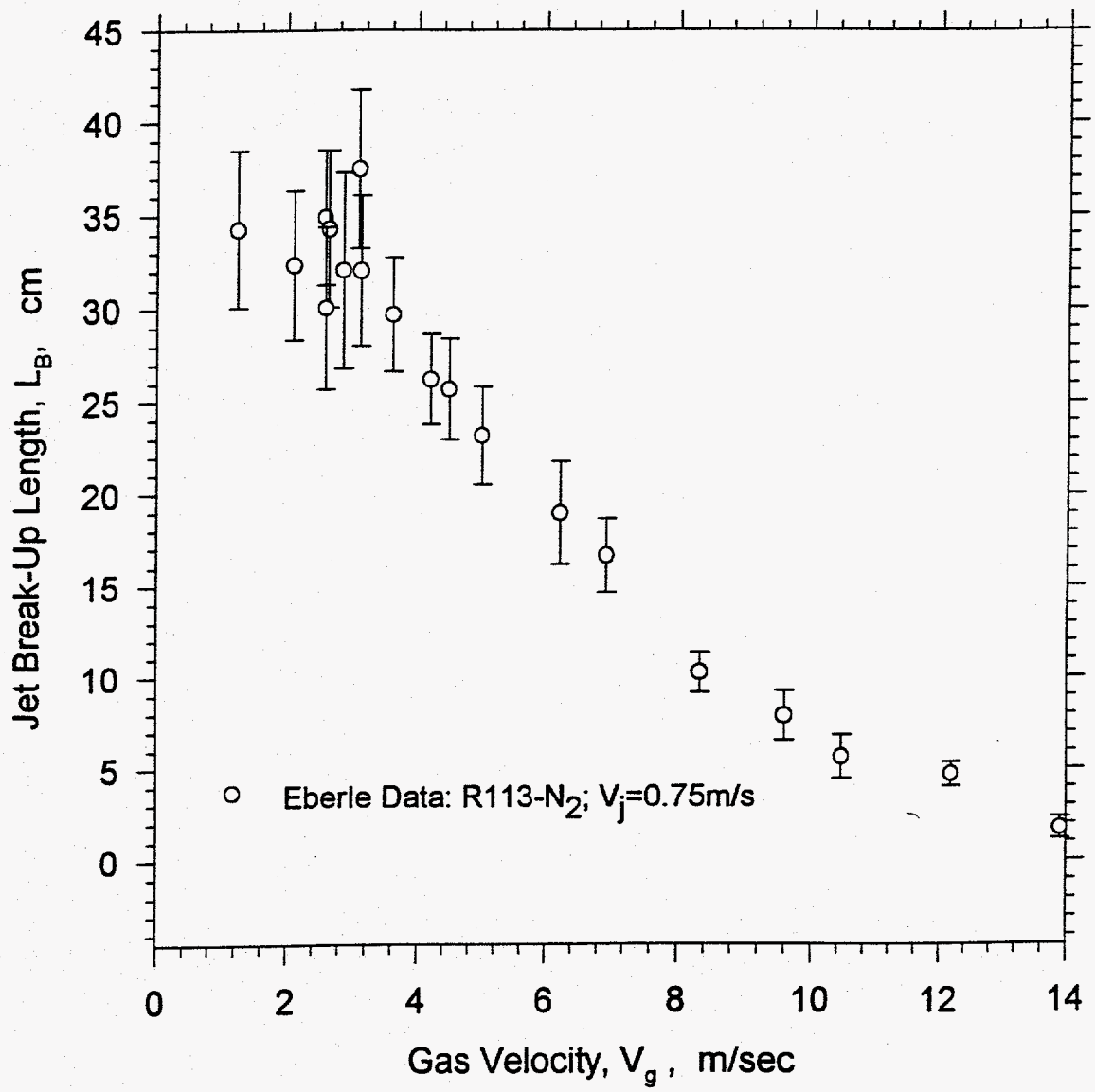

Figure 8. Adiabatic results of L_b versus v_g data including mean and standard error.

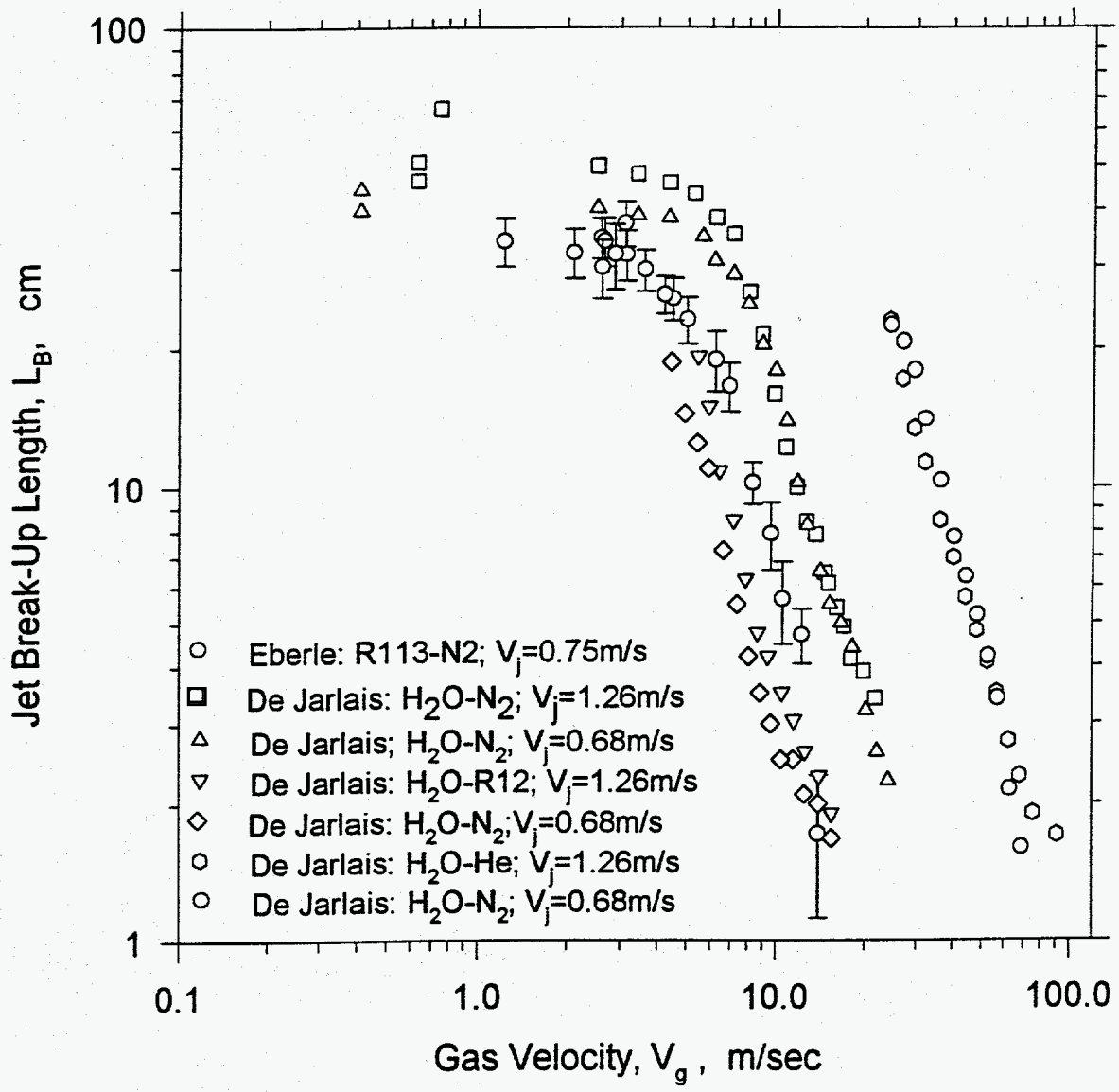

Figure 9. Comparison of Eberle and De Jarlais Adiabatic data.

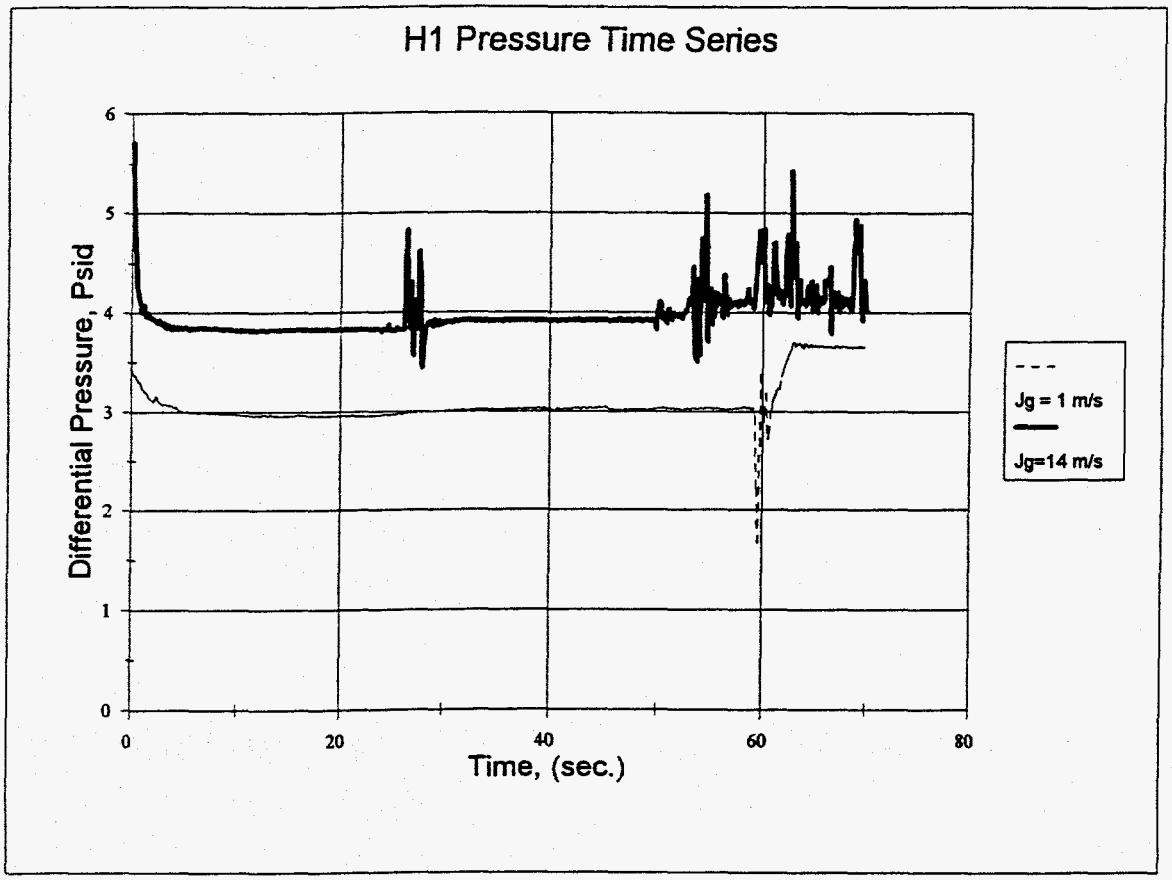

Figure 10. Comparison of adiabatic differential pressure time series.

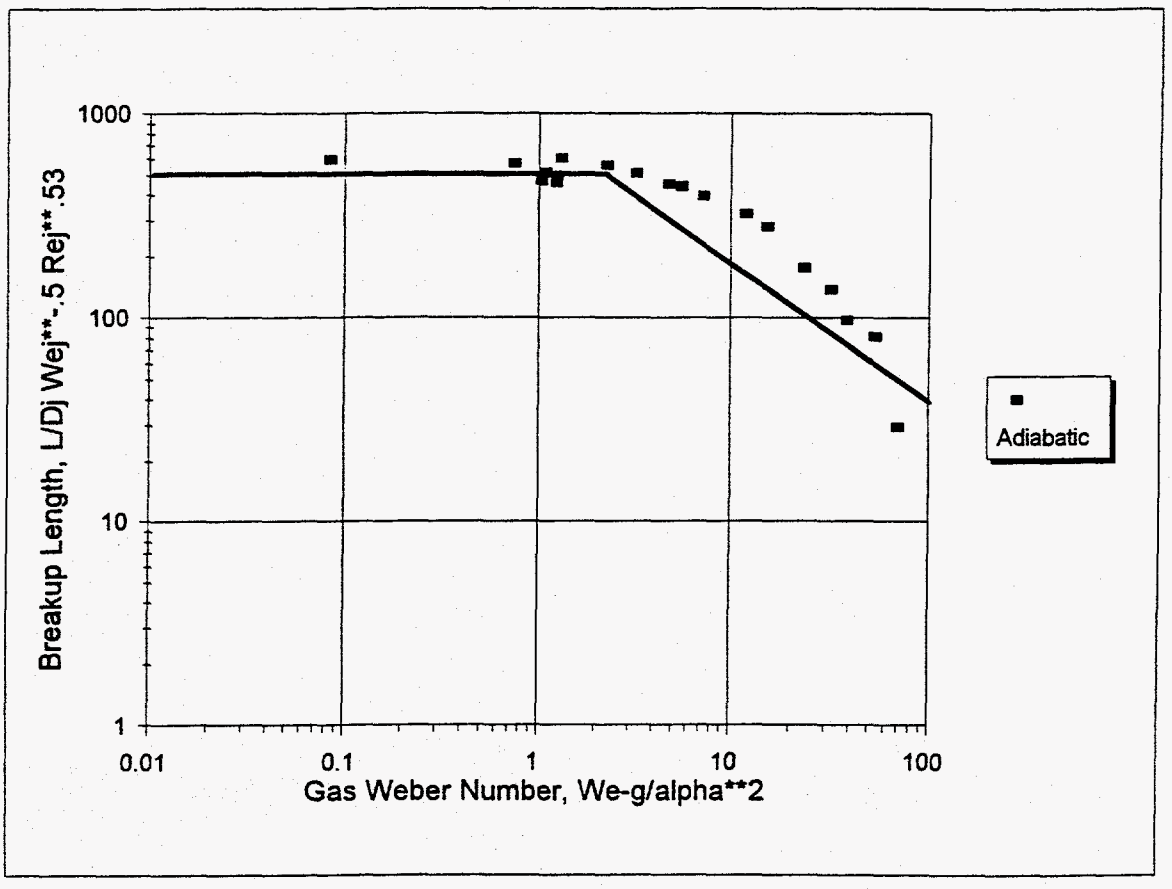

Figure 11. Dimensionless break-up length for Adiabatic data.

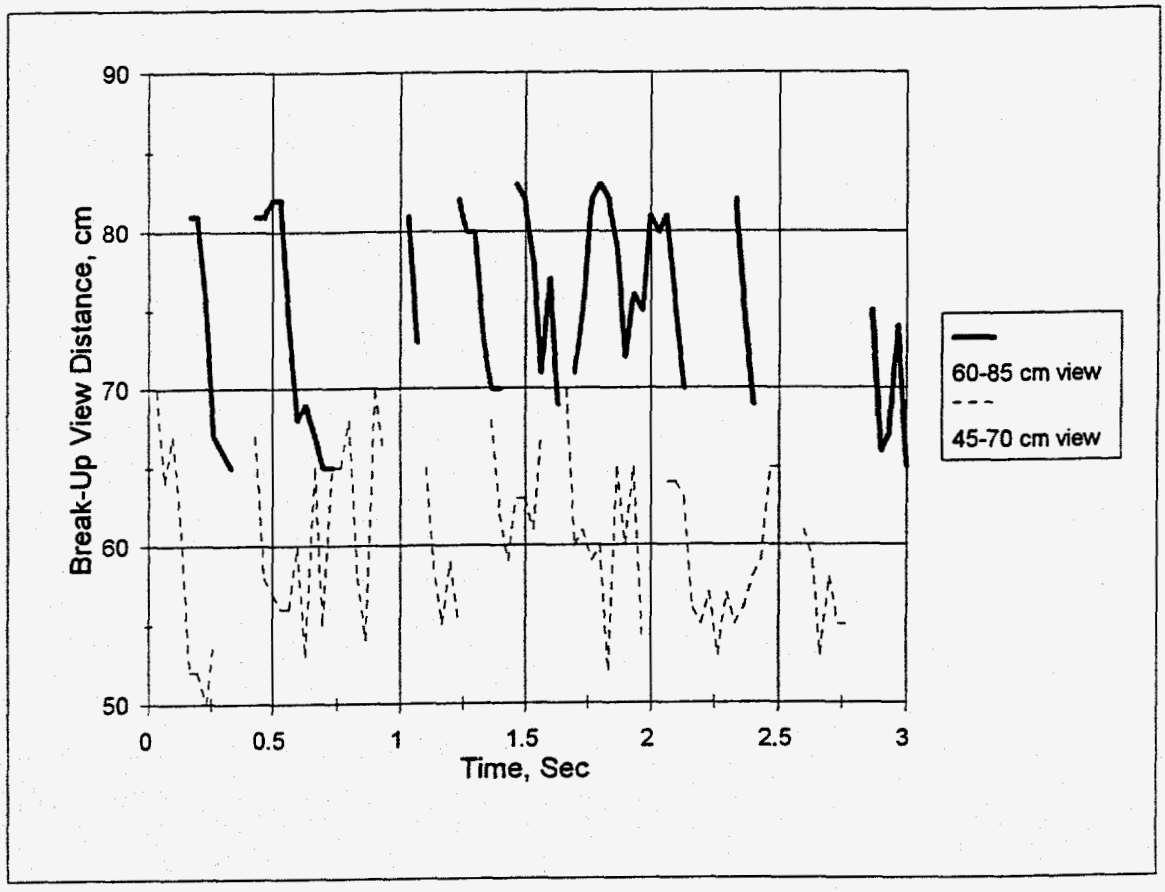

Figure 12. Two break-up filming view windows for H69 data series.

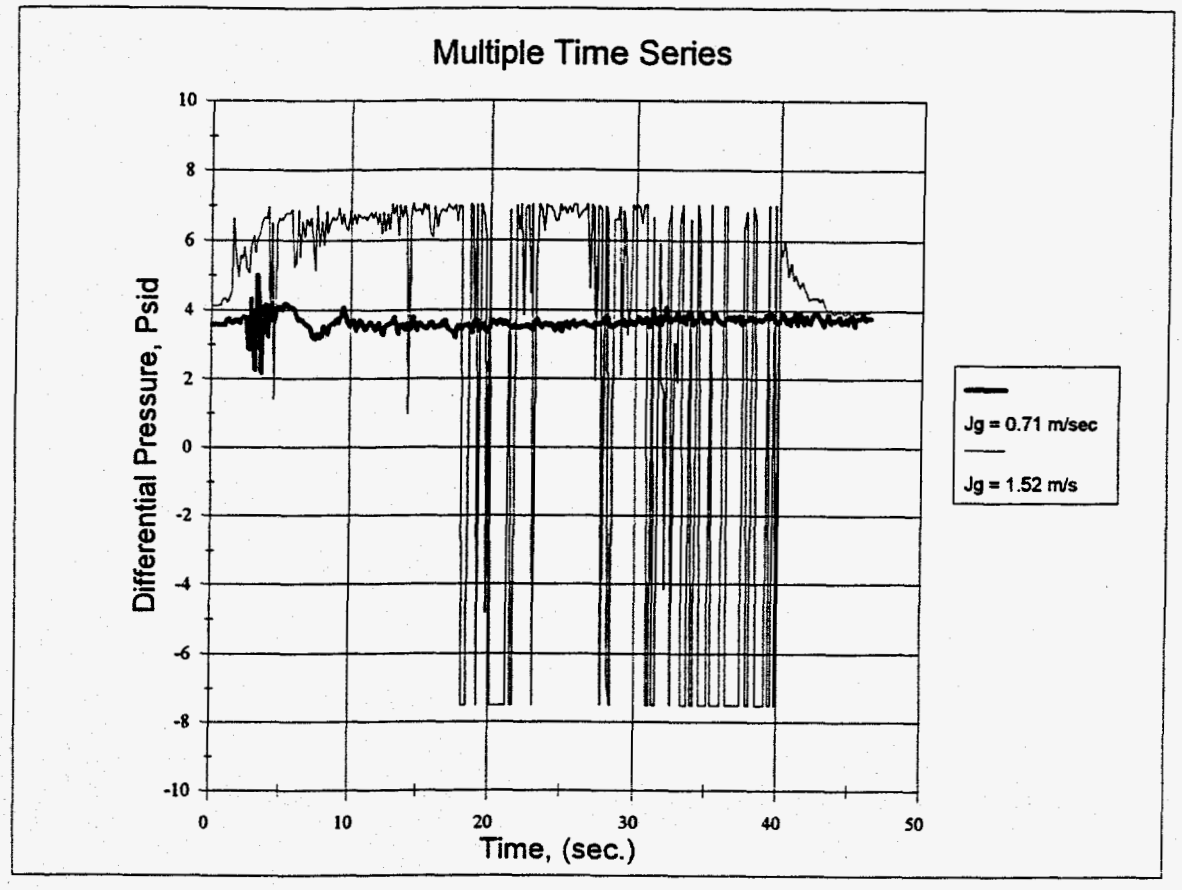

Figure 13. Comparison of diabatic differential pressure time series.

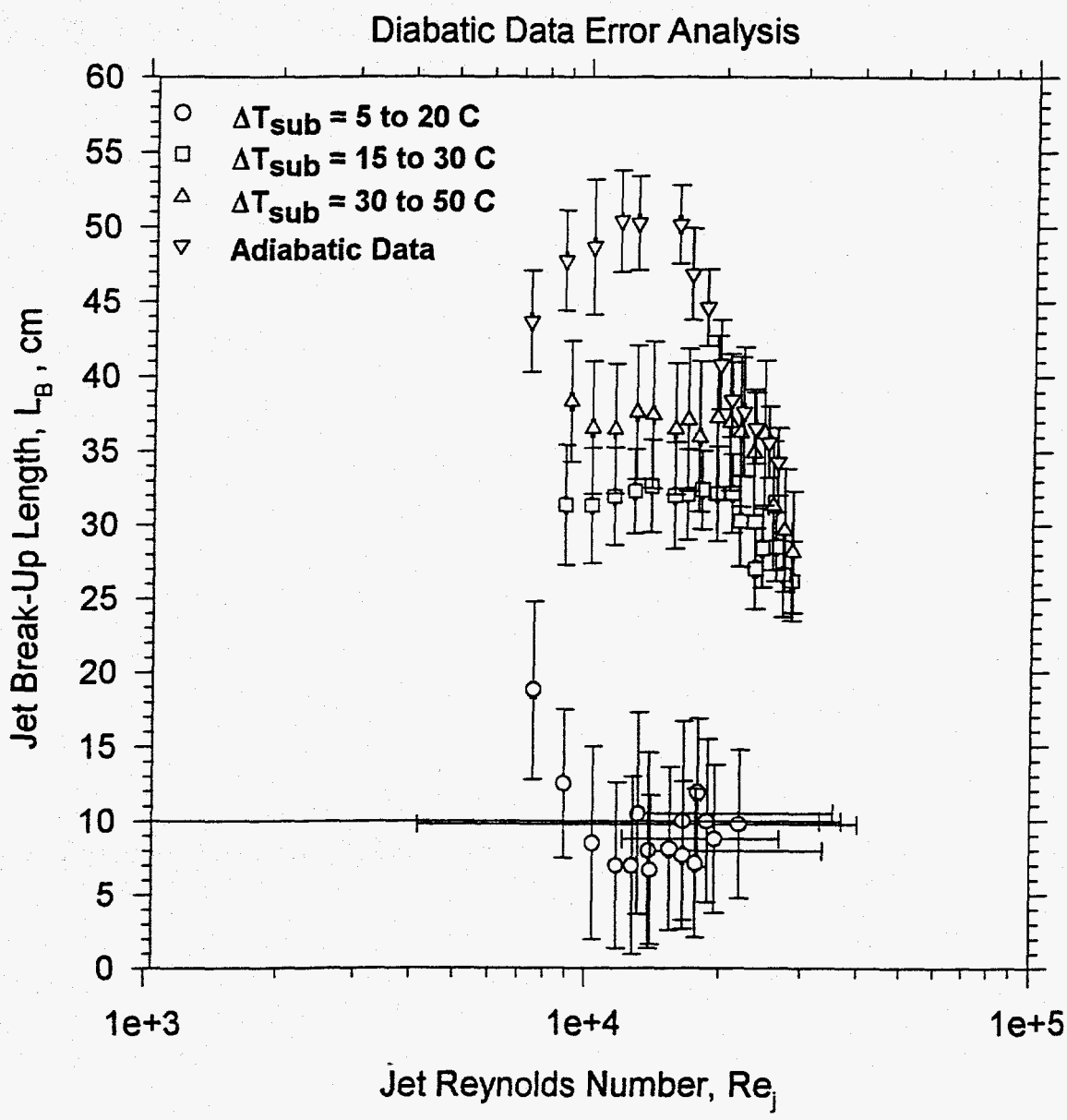

Figure 14. Diabatic error analysis results.

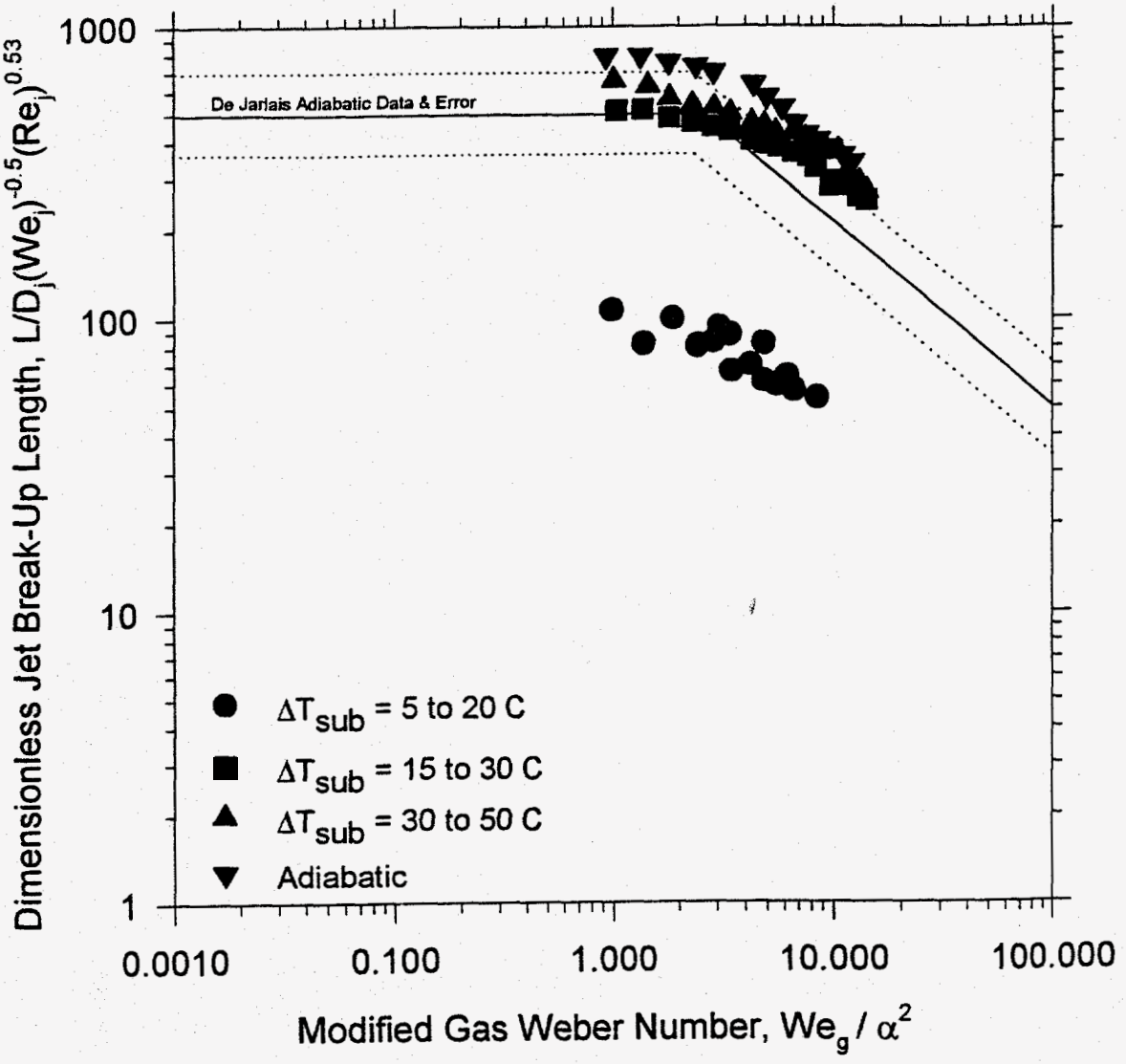

Figure 15. Adiabatic and diabatic data comparison.

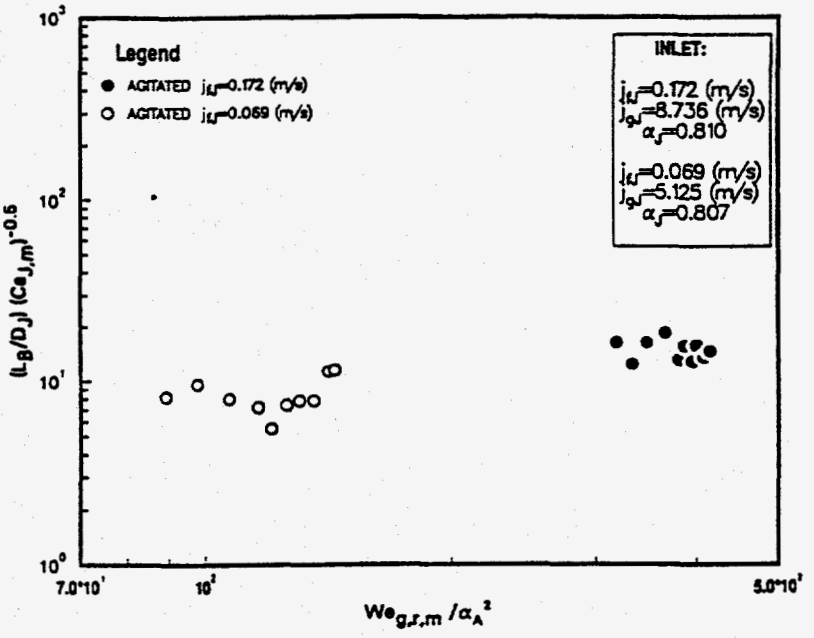

Figure 16. Denten et. al. axial extent data for upflow [23].

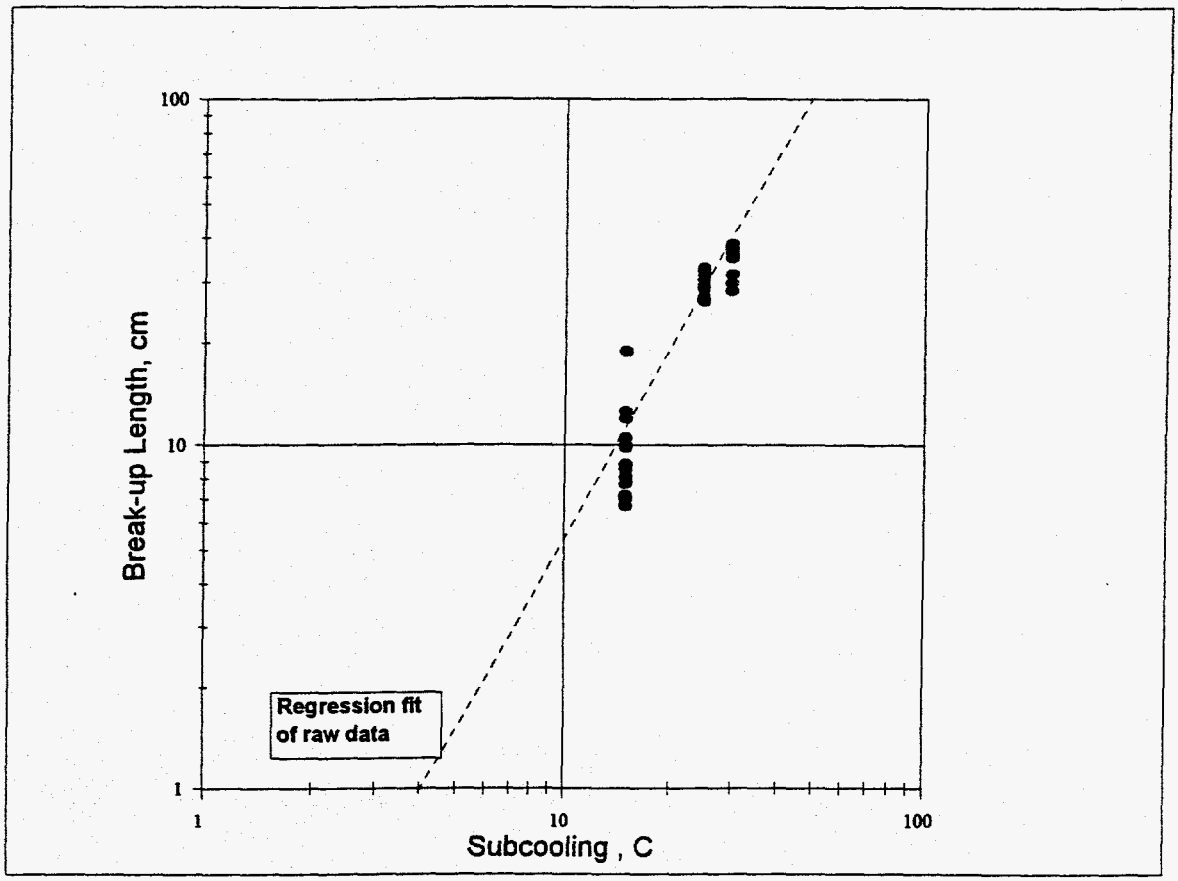

Figure 17. Diabatic break-up length as a function of subcooling.

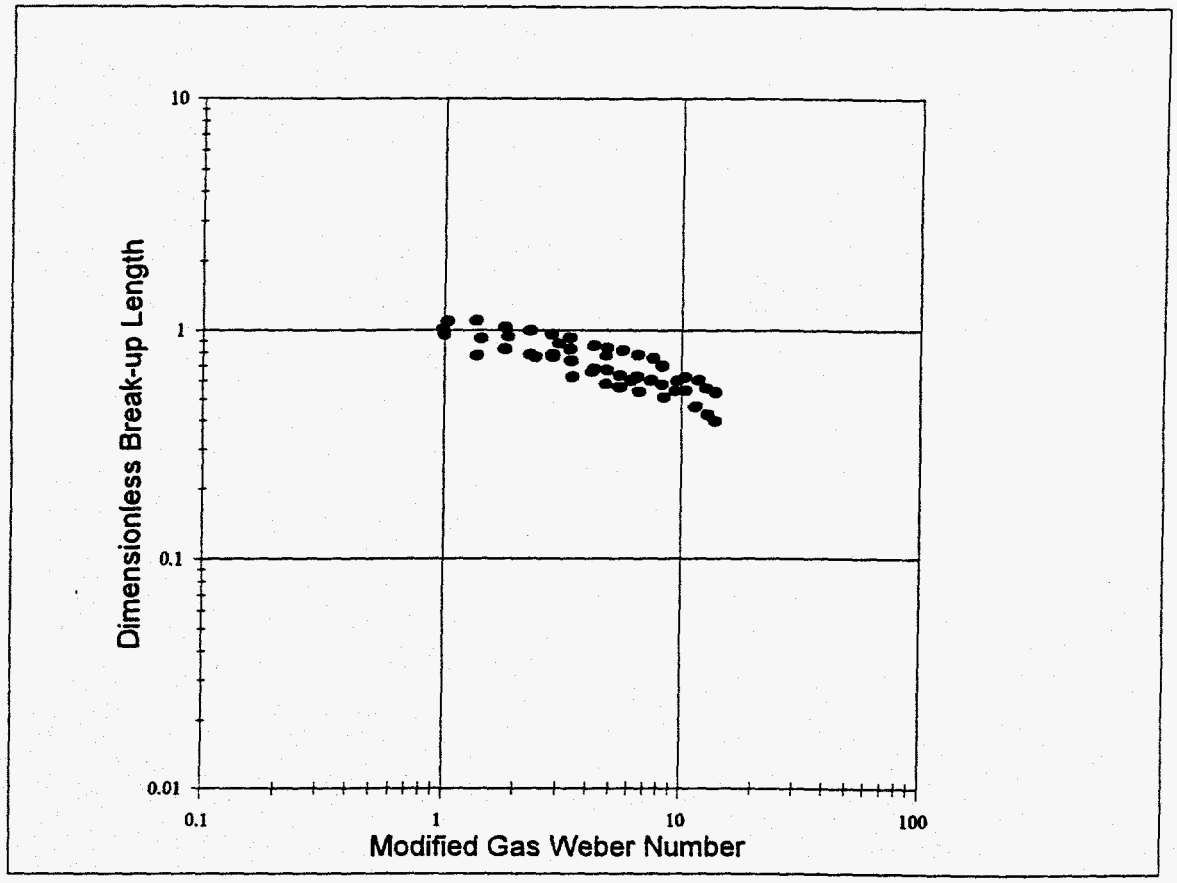

Figure 18. Dimensionless break-up length versus modified gas Weber number.